

Synthesis and antiproliferative activity of some 3-(pyrid-2-yl)-pyrazolines†

Cite this: *Med. Chem. Commun.*, 2013, **4**, 956

Alexander Ciupa,^a Paul A. De Bank,^a Mary F. Mahon,^b Pauline J. Wood^a and Lorenzo Caggiano^{*a}

Received 6th March 2013
Accepted 23rd April 2013

DOI: 10.1039/c3md00077j

www.rsc.org/medchemcomm

The synthesis and antiproliferative activity of eleven 3-(pyrid-2-yl)-pyrazolines in two cancer cell lines are reported. X-ray crystallography was obtained of the lead compound **8i** which was screened in the NCI 60 human tumour cell line and displayed sub-micromolar activity. Cell cycle analysis, *in vitro* tubulin assay and confocal microscopy are also reported and suggest that the lead compound disrupts microtubule formation.

Introduction

Numerous pyrazoline derivatives possess potent biological activities,^{1,2} including antiproliferative,^{3–6} antimalarial⁷ and antibacterial activities.⁸ The inhibition of various processes such as xanthine oxidase,⁹ COX-2,¹⁰ monoamine oxidase^{11–17} and, of particular relevance to the current study, tubulin polymerisation¹⁸ have also been reported (selected examples are shown in Fig. 1).

We have previously reported the synthesis and physico-chemical properties of the simple pyrazoline **8a** ($R^1 = H$, $R^2 =$

Me) and the corresponding oxidised pyrazole derivative, which are “turn on” fluorescent sensors for Cd^{2+} and Zn^{2+} , respectively.¹⁹ Our interests in pyrazolines derived from 2-acetylpyridine **3** originated from possible chelation of ions in these systems by the pyridine nitrogen, the basic pyrazoline nitrogen (N2) and co-ordinating groups (R^2 , Scheme 1). Compounds of this structure have been reported as ligands for gold and display antiproliferative activities.²⁰ In addition, the 3-pyridyl motif would afford compounds with improved pharmacological properties. N1-Substituted 3-(pyrid-2-yl)-pyrazolines display various biological activities, including antitubercular,²¹ antimycobacterial,²² antifungal,²³ anti-inflammatory^{24,25} and antiproliferative^{20,24} activities. We therefore wished to investigate novel compounds of this class and examine their antiproliferative activity.

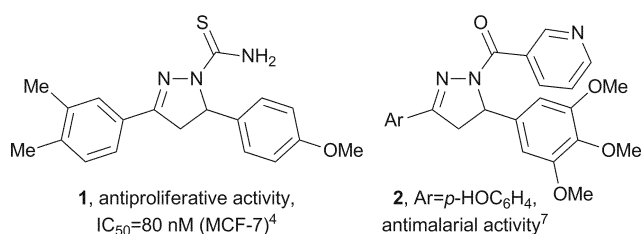
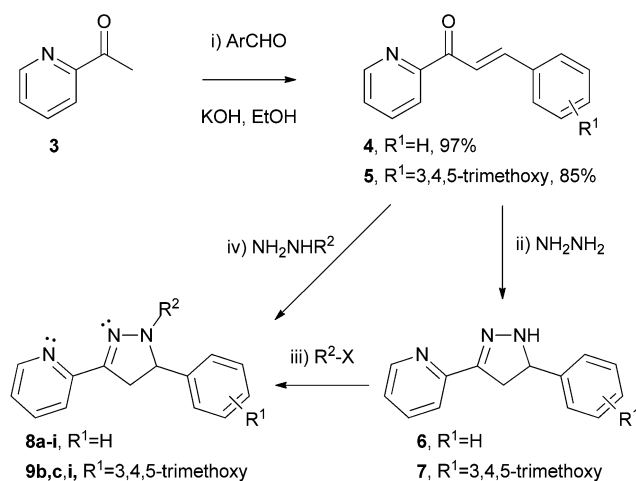


Fig. 1 Examples of biologically active pyrazolines **1** and **2**.

^aMedicinal Chemistry, Department of Pharmacy and Pharmacology, University of Bath, Claverton Down, Bath, BA2 7AY, UK. E-mail: l.caggiano@bath.ac.uk; Fax: +44 (0)1225 386114; Tel: +44 (0)1225 385709

^bX-ray Crystallography Unit, Department of Chemistry, University of Bath, Claverton Down, Bath, BA2 7AY, UK

† Electronic supplementary information (ESI) is available: Experimental procedures, characterisation data, ¹H and ¹³C NMR spectra, HPLC traces and MTS assays for all compounds. In addition, NCI data and cell cycle analysis of compound **8i** together with X-ray crystallography data for pyrazolines **8e** and **8i** are provided. CCDC 926530 and 926531. For ESI and crystallographic data in CIF or other electronic format see DOI: 10.1039/c3md00077j



Scheme 1 Synthesis of 3-(pyrid-2-yl)-pyrazolines **8** and **9** (see Table 1 for R^2 groups and yields).



Results and discussion

Continuing our research interests in pyrazolines derived from 2-acetylpyridine **3**, we synthesised various derivatives following the sequence shown in Scheme 1. Claisen–Schmidt condensation of 2-acetylpyridine **3** with an aromatic aldehyde gave the corresponding chalcone **4** (97%) or **5** (85%) in excellent yields. Treatment with an excess of hydrazine hydrate gave the N–H pyrazoline derivative **6** or **7** which could be characterised by ¹H NMR. Attempts to purify these compounds by silica gel column chromatography however led to decomposition, as was previously observed with similar substrates,^{22,23,26} possibly due to autoxidation.²⁷ Instead, the N–H pyrazolines **6** and **7** were treated directly with the desired electrophile to afford the N-substituted pyrazolines **8** and **9** which could be purified, in a one-pot transformation in good yields.

The N–Me and N–Ph substituted pyrazolines **8a,b** and **9b** were synthesised by reaction of the chalcone **4** or **5** with the commercially available substituted hydrazine NH₂NHMe or NH₂NHPh, affording the corresponding products **8a** (72%),¹⁹ **8b** (49%) or **9b** (34%) directly (iv), Scheme 1). Low yields with arylhydrazines have been previously reported,²⁶ and similar transformations suggest that the reaction proceeds *via* initial 1,2-addition followed by cyclisation and not 1,4-conjugate addition and subsequent cyclisation, which could generate different isomers.^{19,28}

Compounds were examined for antiproliferative activity *in vitro* using the MTS assay²⁹ with human colon carcinoma (HT29) and highly metastatic human breast carcinoma (MDA-MB-231) cell lines. The results are reported as the concentration required to inhibit 50% cell proliferation (IC₅₀) and are shown in Table 1.

The unsubstituted chalcone **4** has been reported to display modest antiproliferative activity in various cancer cell lines.³⁰ Likewise, the 3,4,5-trimethoxy derivative **5** showed good activity in both the cell lines examined in this study (entry 1, Table 1). As can be seen in Table 1, the R² substituent had a great effect on the antiproliferative activity of the pyrazolines. In the C5-phenyl

pyrazoline series **8**, the N–Me derivative **8a** displayed weak activity, which improved two-fold with the N–Ph analogue **8b** (entries 2 and 3). The introduction of an *N*-acetyl group (**8c**), which provides additional Lewis basic sites, resulted in partial loss of activity although it did exhibit some selectivity for the HT29 cell line (entry 4). The trifluoroacetyl analogue **8d**, which has a similar steric requirement as the acetyl but is a much less effective Lewis base, resulted in complete loss of antiproliferative activity in both cell lines (entry 5).

The carbothioamide **1** shown in Fig. 1 displayed potent antiproliferative activity⁴ and similar compounds also show promise.^{5,6} The related derivative **8e** was previously reported to exhibit activity as a gold complex with HeLa and A549 cancer cell lines.²⁰ As the free ligand, however, the carbothioamide **8e** gave poor inhibition of cell growth in the HT29 and MDA-MB-231 cell lines, while the monomethyl analogue **8f** exhibited much improved activities for both cell lines (entries 6 and 7, Table 1).

X-ray crystallography of the carbothioamide **8e** indicated a putative intramolecular H-bond to the basic pyrazoline nitrogen (shown in Fig. 2) and an intermolecular H-bond with the pyridine nitrogen (shown in the ESI[†]). Likewise, the monomethyl derivative **8f** could also possess intramolecular co-ordination to the remaining N–H. Although these interactions are present in the solid state, in aqueous solution competing intermolecular H-bonding to the solvent will undoubtedly occur, affording different conformations such as that observed in co-ordination with gold.²⁰ To investigate further we attempted to generate the dimethyl analogue **8g**, as this would remove the interaction altogether. Attempts to obtain pyrazoline **8g** either by methylation of the carbothioamide **8e** or **8f**, or by reaction of the N–H pyrazoline **6** with dimethylthiocarbonyl chloride, were however unsuccessful as previously observed in similar substrates.²⁶

The effect of an *N*-benzoyl substituent (**8h**) was also investigated and exhibited no observable antiproliferative activity in the two cell lines examined (entry 8, Table 1). Following our

Table 1 Yields and antiproliferative activities against human colon (HT29) and breast (MDA-MB-231) cancer cell lines

Entry	Comp.	R ¹	R ²	Yield ^b (%)	IC ₅₀ ^a (μM)	
					HT29	MDA-MB-231
1	5	3,4,5-OMe	—	85	9.6 ± 0.9	9.7 ± 4.3
2	8a	H	Me	72	115.8 ± 11.6	135 ± 31.2
3	8b	H	Ph	49	53.8 ± 3.94	60.2 ± 19.6
4	8c	H	Ac	72	161.3 ± 21.9	294.1 ± 71.1
5	8d	H	CF ₃ C=O	65	>500	>500
6	8e	H	NH ₂ C=S	67	350.2 ± 42.0	140.5 ± 42.0
7	8f	H	NHMeC=S	89	25.6 ± 4.0	20.7 ± 0.79
8	8h	H	Bz	76	>500	>500*
9	8i	H	3,4,5-Trimethoxy-benzoyl	75	2.53 ± 0.39	0.69 ± 0.10
10	9b	3,4,5-OMe	Ph	34	26.2 ± 3.4	4.36 ± 0.85
11	9c	3,4,5-OMe	Ac	80	>500	52.5 ± 6.5
12	9i	3,4,5-OMe	3,4,5-Trimethoxy-benzoyl	84	22.5 ± 2.50	11.4 ± 0.75
13	Colchicine ^c				0.008 ± 0.001	0.008 ± 0.001

^a IC₅₀ is the concentration that inhibits 50% cell proliferation. Values are the mean from three independent experiments, except * (one), with quadruplicate readings in each. ^b Yield over two steps from the chalcone (steps (ii) and (iii), Scheme 1). ^c Colchicine was used as a positive control.



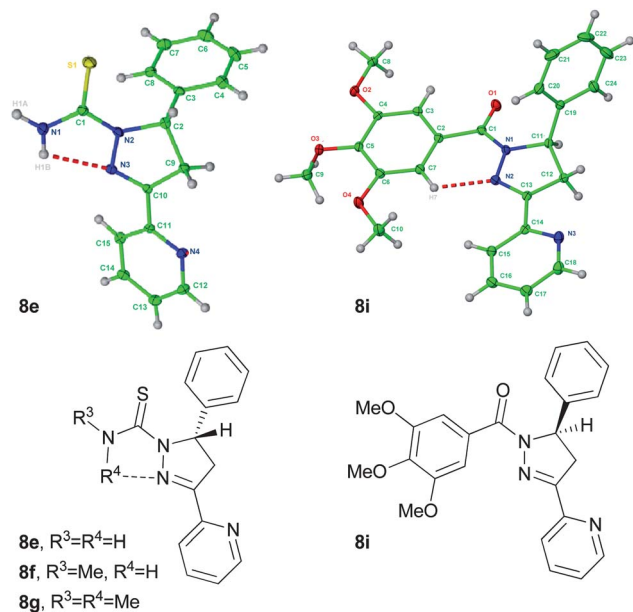


Fig. 2 X-ray crystal structures of pyrazolines **8e** and **8i** with ellipsoids represented at 30% probability.†

previous studies using 3,4,5-trimethoxyphenyl substituents,³¹ which have been shown to play crucial roles in activity,^{32–36} we investigated this substitution pattern in the *N*-benzoyl group. Remarkably, the corresponding 3,4,5-trimethoxybenzoyl derivative **8i** displayed potent activity and selectivity for the highly metastatic human breast carcinoma (MDA-MB-231, entry 9). The X-ray crystal structure of pyrazoline **8i** was also obtained and is shown in Fig. 2. As with pyrazoline **8e**, it shows that in the solid state the amide adopted the *E*-conformation.

Continuing our interest in the 3,4,5-trimethoxyphenyl motif, we investigated the effect of this substitution pattern in three examples in the pyrazoline series **9**. In all three examples, the compounds exhibited increased potency for the MDA-MB-231 cell line, as previously observed with derivative **8i** which also possesses the 3,4,5-trimethoxyaryl motif. The *N*-Ph derivative **9b** was more active in both cell lines than the corresponding *C*5-phenyl analogue **8b** (entries 10 and 3, Table 1). Surprisingly, the *N*-Ac derivative **9c** showed no activity in HT29 (>500 μM), yet exhibited improved activity and selectivity for MDA-MB-231 (52.5 μM) compared to pyrazoline **8c** (entries 11 and 4).

† Both pyrazolines **8e** and **8i** were racemic, but single compounds are shown to represent the structures obtained by X-ray crystallography. Crystal data for pyrazoline **8e**, CCDC 926530. Formula: C₁₅H₁₄N₄S₁. *M* = 282.36, monoclinic. Unit cell parameters: *a* = 9.7950(2) Å, *b* = 14.7280(3) Å, *c* = 10.0360(2) Å. α = 90°, β = 107.768(1)°, γ = 90°, *V* = 1378.74(5) Å³, *T* = 150(2) K, space group *P*2₁/*n*, *Z* = 4, 24456 reflections collected, 3152 independent reflections [*R*(int) = 0.0669]. Final *R* indices [*I* > 2σ(*I*)] *R*₁ = 0.0392 and *wR*₂ = 0.0883. *R* indices (all data) *R*₁ = 0.0608 and *wR*₂ = 0.0979. Crystal data for pyrazoline **8i**, CCDC 926531. Formula: C₂₄H₂₃N₃O₄. *M* = 417.45, orthorhombic. Unit cell parameters: *a* = 6.9770(1) Å, *b* = 22.0950(2) Å, *c* = 26.6010(3) Å. α = 90°, β = 90°, γ = 90°, *V* = 4100.73(8) Å³, *T* = 150(2) K, space group *P*bca, *Z* = 8, 56599 reflections collected, 4679 independent reflections [*R*(int) = 0.0645]. Final *R* indices [*I* > 2σ(*I*)] *R*₁ = 0.0422 and *wR*₂ = 0.0882. *R* indices (all data) *R*₁ = 0.0649 and *wR*₂ = 0.0991.

Table 2 NCI 60 cell line screen of pyrazoline **8i** (NSC 761258)

Panel	Cell line	GI ₅₀ ^a (μM)
Leukemia	CCRF-CEM	2.08
	HL-60(TB)	0.747
	MOLT-4	4.46
	RPMI-8226	66.3
	SR	0.415
Non-small cell Lung	A549/ATCC	0.952
	EKVX	>100
	HOP-62	1.82
	HOP-92	>100
	NCI-H226	1.33
	NCI-H23	3.45
	NCI-H322M	>100
	NCI-H460	0.505
	NCI-H522	0.688
	NCI-H460	0.505
Colon	COLO 205	0.585
	HCC-2998	2.32
	HCT-116	0.586
	HCT-15	0.848
	HT29	0.431
	KM12	0.711
	SW-620	0.567
	SF-268	33.4
	SF-539	1.06
	SNB-19	1.89
Melanoma	SNB-75	0.277
	U251	0.868
	LOX IMVI	1.13
	MALME-3M	>100
	M14	0.801
	MDA-MB-435	0.273
	SK-MEL-2	0.699
	SK-MEL-28	1.51
	SK-MEL-5	0.432
	UACC-257	>100
Ovarian	UACC-62	0.541
	IGROV1	7.13
	OVCAR-3	0.719
	OVCAR-4	5.95
	OVCAR-5	4.01
	OVCAR-8	3.28
	NCI/ADR-RES	0.519
	SK-OV-3	0.762
Renal	786-0	1.54
	A498	0.943
	ACHN	4.29
	CAKI-1	0.493
	RXF 393	1.03
	SN12C	3.53
	TK-10	>100
	UO-31	5.01
	PC-3	>100
	DU-145	4.26
Breast	MCF7	0.324
	MDA-MB-231/ATCC	0.989
	HS 578T	9.18
	BT-549	5.13
	T-47D	>100
MDA-MB-468	0.417	

^a GI₅₀ is concentration required to inhibit growth by 50% as defined by the National Cancer Institute (NCI).



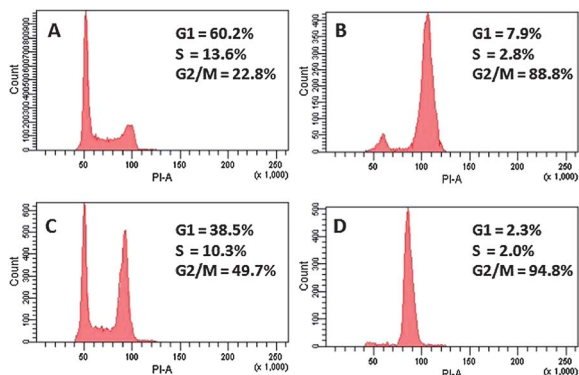


Fig. 3 Cell cycle analysis. (A) HT29 cells only, (B) HT29 + colchicine (100 nM), (C) HT29 + **8i** (1 μM), and (D) HT29 + **8i** (5 μM).

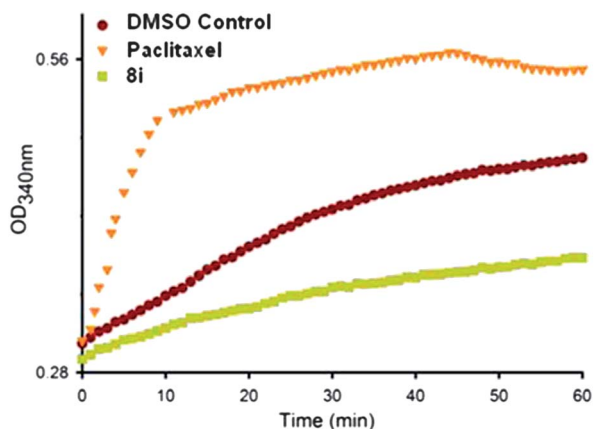


Fig. 4 *In vitro* tubulin polymerisation assay. Paclitaxel (5 μM) and pyrazoline **8i** (20 μM).

Incorporating the 3,4,5-trimethoxy-substitution in both the C5-aryl and N1-benzoyl positions of the pyrazoline ring (**9i**) did not further improve activity compared to compound **8i** (entries 12 and 9). On the basis of these preliminary investigations, compound **8i** was selected for further evaluation by the National Cancer Institute (NCI) and the results are shown in Table 2.

Pyrazoline **8i** (NSC 761258) displayed promising GI₅₀ values across the NCI 60 human tumour cell line panel and exhibited sub-micromolar activity in a range of cancer cell lines, including the multidrug resistant ovarian cell line NCI/ADR-RES (0.519 μM). Also of interest is that one of the most susceptible ovarian cancer cell lines, OVCAR-3, is particularly sensitive to tubulin disruptors,³⁷ suggesting that pyrazoline **8i** may be inhibiting cell proliferation through the disruption of tubulin. Although COMPARE analysis of the NCI 60 cancer cell line data did not afford strong correlations with compounds of known biological activity, drugs which inhibit the polymerization of tubulin did feature (see ESI†).

To investigate potential interaction with tubulin dynamics, cell cycle analysis was performed with HT29 cells with pyrazoline **8i** and colchicine, a known inhibitor of microtubule polymerisation. Cell cycle analysis was performed three times and the results shown in Fig. 3 are representative of the complete study (shown in the ESI†). The presence of 100 nM of colchicine

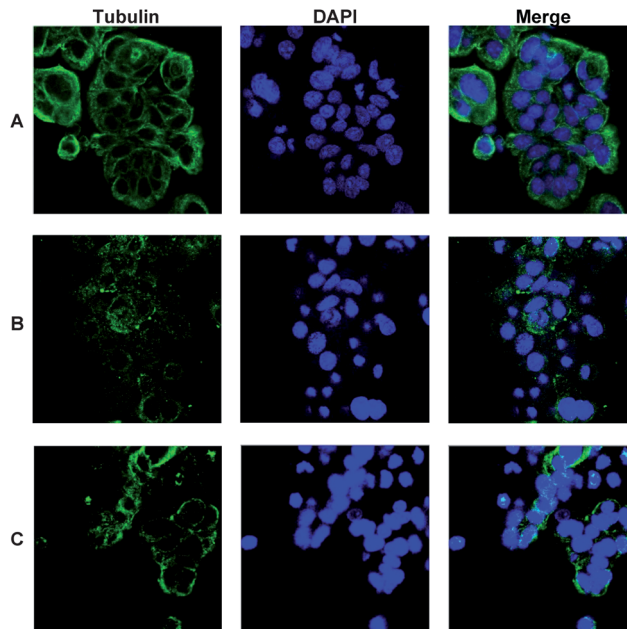


Fig. 5 Confocal microscopy showing tubulin, Dm1a (green) and DNA, DAPI (blue). (A) HT29 cells only, (B) HT29 + colchicine (100 nM) and (C) HT29 + **8i** (5 μM).

led to cell cycle arrest in the G2/M phase, shown in Fig. 3B. In the presence of pyrazoline **8i** at 1 μM (Fig. 3C) and 5 μM (Fig. 3D), 50% and 95% respectively of the cells also arrested in G2/M phase, suggesting that pyrazoline **8i** affects microtubule polymerisation.

To examine this interaction an *in vitro* tubulin polymerisation assay was performed in the presence of pyrazoline **8i** (20 μM) or paclitaxel (5 μM), which is known to polymerise microtubule formation. As can be seen in Fig. 4, the presence of paclitaxel led to an increased optical density (OD) compared to the control experiment, due to increased microtubule formation. The presence of pyrazoline **8i** however gave a lower OD reading than the control, implying that pyrazoline **8i** inhibits microtubule polymerisation and is consistent with the cell cycle analysis.

Confocal microscopy was performed on HT29 cells to visualise the effects of pyrazoline **8i** in microtubule formation, using Dm1a tubulin antibodies (Fig. 5). The effects of 100 nM colchicine, which inhibits microtubule polymerisation, can be seen in Fig. 5B, which contains much less tubulin compared to the control experiment (Fig. 5A). Likewise, compared to the control there is less tubulin present in cells treated with 5 μM pyrazoline **8i** (Fig. 5C), which again supports the data obtained from the cell cycle analysis and *in vitro* tubulin polymerisation assay that pyrazoline **8i** disrupts microtubule formation. The results are consistent with previous reports of similar compounds which were also shown to interfere with microtubule assembly.¹⁸

Conclusions

In conclusion, we report the two-step synthesis of some 3-(pyrid-2-yl)-pyrazolines and their antiproliferative activities. The lead pyrazoline **8i** was selected from this preliminary study and



further investigated against the NCI 60 cancer cell line (NSC 761258) and exhibits sub-micromolar activity in a number of cell lines. The mode of action was explored by cell cycle analysis, *in vitro* microtubule assembly assay and confocal microscopy with α -tubulin antibody Dm1a which suggest that the novel compound **8i** inhibits microtubule polymerisation.

The promising antiproliferative activity of 3-(pyrid-2-yl)-pyrazoline **8i** and the ease of its synthesis provide the potential for further development, which is currently under investigation and will be reported in due course.

Acknowledgements

We wish to thank Dr Timothy J. Woodman, Dr Anneke Lubben and Dr Adrian Rogers (University of Bath) for their assistance with the NMR, mass spectra and confocal spectroscopy, respectively. We also wish to thank Dr Andrew Chalmers for the antibodies used in the confocal experiments and to Cancer Research at Bath (CR@B) for funding the confocal imaging. We are extremely grateful to the National Cancer Institute (NCI) for conducting the *in vitro* testing and the University of Bath for providing a studentship for AC. We also wish to acknowledge RCUK and the University of Bath for the fellowship to LC.

Notes and references

- M. Abdel-Aziz and A. M. Gamal-Eldeen, *Pharm. Biol.*, 2009, **47**, 854–863.
- M. R. Shaaban, A. S. Mayhoub and A. M. Farag, *Expert Opin. Ther. Pat.*, 2012, **22**, 253–291.
- S. A. F. Rostom, M. H. Badr, H. A. Abd El Razik, H. M. A. Ashour and A. E. Abdel Wahab, *Arch. Pharm. Chem. Life Sci.*, 2011, **344**, 572–587.
- P.-C. Lv, H.-Q. Li, J. Sun, Y. Zhou and H.-L. Zhu, *Bioorg. Med. Chem.*, 2010, **18**, 4606–4614.
- B. Insuasty, L. Chamizo, J. Muñoz, A. Tigreros, J. Quiroga, R. Abonía, M. Nogueras and J. Cobo, *Arch. Pharm. Chem. Life Sci.*, 2012, **345**, 275–286.
- A.-S. S. Hamad Elgazwy, D. H. S. Soliman, S. R. Atta-Allah and D. A. Ibrahim, *Chem. Cent. J.*, 2012, **6**, 50.
- B. N. Acharya, D. Saraswat, M. Tiwari, A. K. Shrivastava, R. Ghorpade, S. Bapna and M. P. Kaushik, *Eur. J. Med. Chem.*, 2010, **45**, 430–438.
- P. M. Sivakumar, S. Ganesan, P. Veluchamy and M. Doble, *Chem. Biol. Drug Des.*, 2010, **76**, 407–411.
- K. Nepali, G. Singh, A. Turan, A. Agarwal, S. Sapra, R. Kumar, U. C. Banerjee, P. K. Verma, N. K. Satti, M. K. Gupta, O. P. Suri and K. L. Dhar, *Bioorg. Med. Chem.*, 2011, **19**, 1950–1958.
- R. Fioravanti, A. Bolasco, F. Manna, F. Rossi, F. Orallo, F. Ortuso, S. Alcaro and R. Cirilli, *Eur. J. Med. Chem.*, 2010, **45**, 6135–6138.
- R. Cirilli, R. Ferretti, B. Gallinella, L. Turchetto, A. Bolasco, D. Secci, P. Chimenti, M. Pierini, V. Fares, O. Befani and F. La Torre, *Chirality*, 2004, **16**, 625–636.
- N. Gökhan-Kelekçi, S. Yabanoğlu, E. Küpeli, U. Salgin, Ö. Özgen, G. Uçar, E. Yeşilada, E. Kendi, A. Yeşilada and A. A. Bilgin, *Bioorg. Med. Chem.*, 2007, **15**, 5775–5786.
- A. Sahoo, S. Yabanoglu, B. N. Sinha, G. Ucar, A. Basu and V. Jayaprakash, *Bioorg. Med. Chem. Lett.*, 2010, **20**, 132–136.
- F. Chimenti, A. Bolasco, F. Manna, D. Secci, P. Chimenti, O. Befani, P. Turini, V. Giovannini, B. Mondovi, R. Cirilli and F. La Torre, *J. Med. Chem.*, 2004, **47**, 2071–2074.
- F. Chimenti, E. Maccioni, D. Secci, A. Bolasco, P. Chimenti, A. Granese, O. Befani, P. Turini, S. Alcaro, F. Ortuso, R. Cirilli, F. La Torre, M. C. Cardia and S. Distinto, *J. Med. Chem.*, 2005, **48**, 7113–7122.
- F. Chimenti, A. Bolasco, F. Manna, D. Secci, P. Chimenti, A. Granese, O. Befani, P. Turini, S. Alcaro and F. Ortuso, *Chem. Biol. Drug Des.*, 2006, **67**, 206–214.
- R. Fioravanti, A. Bolasco, F. Manna, F. Rossi, F. Orallo, M. Yáñez, A. Vitali, F. Ortuso and S. Alcaro, *Bioorg. Med. Chem. Lett.*, 2010, **20**, 6479–6482.
- M. Abdel-Aziz, O. M. Aly, S. S. Khan, K. Mukherjee and S. Bane, *Arch. Pharm. Chem. Life Sci.*, 2012, **345**, 535–548.
- A. Ciupa, M. F. Mahon, P. A. De Bank and L. Caggiano, *Org. Biomol. Chem.*, 2012, **10**, 8753–8757.
- S. Wang, W. Shao, H. Li, C. Liu, K. Wang and J. Zhang, *Eur. J. Med. Chem.*, 2011, **46**, 1914–1918.
- S. G. Kini, A. R. Bhat, B. Bryant, J. S. Williamson and F. E. Dayan, *Eur. J. Med. Chem.*, 2009, **44**, 492–500.
- M. G. Mamolo, D. Zampieri, V. Falagiani, L. Vio and E. Banfi, *Il Farmaco*, 2001, **56**, 593–599.
- M. G. Mamolo, D. Zampieri, V. Falagiani, L. Vio and E. Banfi, *Il Farmaco*, 2003, **58**, 315–322.
- S. M. Sondhi, S. Kumar, N. Kumar and P. Roy, *Med. Chem. Res.*, 2012, **21**, 3043–3052.
- B. P. Bandgar, L. K. Adsul, H. V. Chavan, S. S. Jalde, S. N. Shringare, R. Shaikh, R. J. Meshram, R. N. Gacche and V. Masand, *Bioorg. Med. Chem. Lett.*, 2012, **22**, 5839–5844.
- C. D. Cox, M. J. Breslin and B. J. Mariano, *Tetrahedron Lett.*, 2004, **45**, 1489–1493.
- A. L. Baumstark, M. Dotrong and P. C. Vasquez, *Tetrahedron Lett.*, 1987, **28**, 1963–1966.
- Z.-L. Gong, L.-W. Zheng, B.-X. Zhao, D.-Z. Yang, H.-S. Lv, W.-Y. Liu and S. Lian, *J. Photochem. Photobiol.*, 2010, **209**, 49–55.
- A. H. Cory, T. C. Owen, J. A. Barltrop and J. G. Cory, *Cancer Commun.*, 1991, **3**, 207–212. MTS is 3-(4,5-dimethylthiazol-2-yl)-5-(3-carboxymethoxyphenyl)-2-(4-sulfophenyl)-2H-tetrazolium.
- L. Mishra, R. Sinha, H. Itokawa, K. F. Bastow, Y. Tachibana, Y. Nakanishi, N. Kilgore and K.-H. Lee, *Bioorg. Med. Chem.*, 2001, **9**, 1667–1671.
- A. Ciupa, N. J. Griffiths, S. K. Light, P. J. Wood and L. Caggiano, *Med. Chem. Commun.*, 2011, **2**, 1011–1015.
- K. Gaukroger, J. A. Hadfield, N. J. Lawrence, S. Nolan and A. T. McGown, *Org. Biomol. Chem.*, 2003, **1**, 3033–3037.
- T. M. Beale, R. M. Myers, J. W. Shearman, D. S. Charnock-Jones, J. D. Brenton, F. V. Gergely and S. V. Ley, *Med. Chem. Commun.*, 2010, **1**, 202–208.



- 34 A. Kamal, Y. V. V. Srikanth, T. B. Shaik, M. N. A. Khan, M. Ashraf, M. K. Reddy, K. A. Kumar and S. V. Kalivendi, *Med. Chem. Commun.*, 2011, **2**, 819–823.
- 35 A. Kamal, J. S. Reddy, M. J. Ramaiah, D. Dastagiri, E. V. Bharathi, M. V. P. Sagar, S. N. C. V. L. Pushpavalli, P. Ray and M. Pal-Bhadra, *Med. Chem. Commun.*, 2010, **1**, 355–360.
- 36 A. Kamal, A. Viswanath, M. J. Ramaiah, J. N. S. R. C. Murty, F. Sultana, G. Ramakrishna, J. R. Tamboli, S. N. C. V. L. Pushpavalli, D. Pal, C. Kishor, A. Addlagatta and M. P. Bhadra, *Med. Chem. Commun.*, 2012, **3**, 1386–1392.
- 37 R. H. Shoemaker, *Nat. Rev. Cancer*, 2006, **6**, 813–823.

